
OXFORD CENTRE FOR COLLABORATIVE APPLIED MATHEMATICS

Report Number 11/46

# A two-compartment mechanochemical model of the roles of transforming growth factor $\beta$ and tissue tension in dermal wound healing

by

**Kelly E. Murphy, Cameron L. Hall, Philip K. Maini, Scott W. McCue, and D.L. Sean McElwain**


**Oxford Centre for Collaborative Applied Mathematics**
**Mathematical Institute**
**24 - 29 St Giles'**
**Oxford**
**OX1 3LB**
**England**

# A two-compartment mechanochemical model of the roles of transforming growth factor $\beta$ and tissue tension in dermal wound healing

Kelly E. Murphy[a,b,*], Cameron L. Hall[c], Scott W. McCue[a,b], D.L. Sean McElwain[a,b]

[a] *Discipline of Mathematical Sciences, Queensland University of Technology, GPO Box 2434, Brisbane QLD 4001, Australia*

[b] *Tissue Repair and Regeneration Program, Institute of Health and Biomedical Innovation, Queensland University of Technology, GPO Box 2434, Brisbane QLD 4001, Australia*

[c] *Oxford Centre for Collaborative and Applied Mathematics, Mathematical Institute, University of Oxford, 24-29 St Giles', Oxford OX1 3LB, UK*

**Abstract**

The repair of dermal tissue is a complex process of interconnected phenomena, where cellular, chemical and mechanical aspects all play a role, both in an autocrine and in a paracrine fashion. Recent experimental results have shown that transforming growth factor$-\beta$ (TGF$\beta$) and tissue mechanics play roles in regulating cell proliferation, differentiation and the production of extracellular materials. We have developed a 1D mathematical model that considers the interaction between the cellular, chemical and mechanical phenomena, allowing the combination of TGF$\beta$ and tissue stress to inform the activation of fibroblasts to myofibroblasts. Additionally, our model incorporates the observed feature of residual stress by considering the changing zero-stress state in the formulation for effective strain. Using this model, we predict that the continued presence of TGF$\beta$ in dermal wounds will produce

*Corresponding author
*Email address:* kelly.murphy@qut.edu.au (Kelly E. Murphy)

contractures due to the persistence of myofibroblasts; in contrast, early elimination of TGF$\beta$ significantly reduces the myofibroblast numbers resulting in an increase in wound size. Similar results were obtained by varying the rate at which fibroblasts differentiate to myofibroblasts and by changing the myofibroblast apoptotic rate. Taken together, the implication is that elevated levels of myofibroblasts is the key factor behind wounds healing with excessive contraction, suggesting that clinical strategies which aim to reduce the myofibroblast density may reduce the appearance of contractures.
*Keywords:* biomechanics, morphoelasticity, zero stress states, myofibroblasts

---

## 1. Introduction

Severance of the dermal layer triggers a repair response that fails to regenerate the original architecture of the tissue. Consequently the final outcome, scar tissue, is both biologically and mechanically inferior to the unwounded dermis. The overall healing process is complex and can be described in terms of four overlapping but well-defined stages of wound repair: haemostasis, inflammation, proliferation and lastly, remodelling and scar formation (Moulin et al., 2004; Enoch et al., 2006).

Haemostasis is the initial response to injury, beginning with arresting blood flow by vasoconstriction. Platelets aggregate at the perforations in the vasculature, forming a thrombus. This establishes a fibrin clot in the wound space that acts as a temporary scaffold over which cells migrate. In addition, growth factors such as thrombin (Majno and Joris, 2004), platelet-derived growth factor (PDGF) (Singer and Clark, 1999) and transforming growth factors $\beta_1$ and $\beta_2$ (TGF$\beta$) (Singer and Clark, 1999) are released, attracting macrophages into the wound space and initiating the inflammatory response.

Inflammation is triggered irrespective of the presence of infection. Leukocytes such as macrophages, mast cells and neutrophils migrate into the region, phagocytose damaged tissue and detritus and remove foreign bodies. These cells release large quantities of growth factors including TGF$\beta$, which is one of the main regulatory growth factors in dermal repair. TGF$\beta$ is implicated in the stimulation of angiogenesis, the formation of granulation tissue, the regulation of fibroblast collagen synthesis (Roberts et al., 1992; Murata et al., 1997; Rhett et al., 2008) and the development of fibroplasia; later in the wound healing process it also helps to determine the final appearance of the scar (Ferguson and O'Kane, 2004). Late in the inflammatory stage TGF$\beta$ initiates the recruitment of fibroblasts, the main cell type in dermal repair, into the lesion. This migration of fibroblasts corresponds to the beginning of the proliferative phase.

In the proliferative stage, the fibroblasts migrate over the fibrin framework simultaneously replacing it with a collagen lattice and thereby restoring the extracellular matrix (ECM) within the wound. Endothelial cells, responsible for the vascularisation of scar tissue, use the ECM as a scaffold for the new vessels. Hence, angiogenesis occurs concurrently with proliferation. Fibroblasts also modulate into their active, contractile phenotype, the myofibroblast, and together fibroblasts and myofibroblasts effect wound contraction through physically exerting traction on the collagen fibres and through remodelling the collagen lattice. Experimental results for rat dermal repair have shown that for this contractile phase, the wound size can be modelled by an exponential decay function (McGrath and Simon, 1983).

Previously, it was known that the activation of fibroblasts to myofibroblasts was TGF$\beta$-dependent (Desmouliere et al., 1993). However, more recent experimental research by Gabbiani (2003), Hinz (2007, 2009, 2010) and others have shown that mechanical tension is also required to initiate and

maintain this phenotypic change (Wells and Discher, 2008; Wipff and Hinz, 2009; Eckes et al., 2010). This differentiation is a two-stage process. Firstly, mechanical tension, the result of the compaction by tractional forces, initiates the activation to proto-myofibroblasts, the precursors to myofibroblasts (Hinz and Gabbiani, 2003). Proto-myofibroblasts are characterised by mature focal adhesions and immature actin filaments (Gabbiani, 2003). Further stimulation by mechanical tension and TGF$\beta$ induces the transformation of proto-myofibroblasts to myofibroblasts. Myofibroblasts are distinguished from proto-myofibroblasts by the presence of stress fibres in their cytosol in the form of $\alpha$-smooth muscle actin ($\alpha$-SMA) and supermature focal adhesions (Hinz and Gabbiani, 2003). In addition, myofibroblasts are thought to perform the majority of wound contraction, while fibroblasts primarily synthesise and remodel the local collagen network.

Once wound closure is complete the scar becomes relatively avascular and myofibroblasts and leukocytes are no longer present. It is speculated that myofibroblasts undergo apoptosis (Moulin et al., 2004). Fibroblasts remain, performing further ECM remodelling that increases the tensile strength of the scar tissue. The process of scar maturation can last for months or even years following injury (Majno and Joris, 2004).

It is our purpose to develop a mathematical model that captures the essential features of the proliferative stage of dermal wound repair and, recognising the importance of both chemical and mechanical signals within the wound healing process, we consider a mechanochemical representation.

The majority of mechanochemical models for dermal repair, such as those of Olsen et al. (1995, 1996, 1997, 1998, 1999), Tracqui et al. (1995), Tranqui and Tracqui (2000), Javierre et al. (2009) and Vermolen and Javierre (2010), are fundamentally based on the seminal work of Tranquillo and Murray (1992) who considered a linear viscoelastic tissue framework. How-

ever, this is appropriate only for small deformations and in human dermal wounds 20-30% of closure is associated with mechanical contraction while in murine dermal wounds this can be up to 80% (Tranquillo and Murray, 1992; Farahani and Kloth, 2008). Clearly, the deformations that occur in dermal wound healing are not always small, and so Tranquillo and Murray's preliminary mechanical framework is unsuitable. In addition, this model does not capture the permanent contraction observed experimentally unless a permanent chemical mediator with a static distribution is invoked.

In the present study, we develop an ordinary differential equation (ODE) model that incorporates the most important features of wound closure and that allows for large tissue displacements.

In the next section, we discuss the only other two-compartment morphoelastic model for dermal repair, which was developed by Cook (1995). We then describe our mathematical representation of dermal wound healing in Section 3, and discuss parameter estimation, a crucial aspect of computational biology. In Section 4, we examine the model predictions and validate the model against experimental results for wound closure. Finally, in Section 5, we discuss the implications of our results and describe possible extensions of the model.

## 2. The Cook Model

We build upon the work of Cook (1995), who developed an ODE mechanochemical model for dermal repair that accounts for the permanent deformations and contraction of the tissue during healing. This approach employed the idea of a zero stress state, which is defined as a state in which each element of the tissue is unstressed (Goriely and Ben Amar, 2007; Hall, 2009). The zero stress state is necessarily defined locally, as it may not be possible to

find a compatible deformation of the entire tissue where every point is simultaneously at zero stress. However, it is still possible to develop a consistent theory with only locally-defined zero stress states by using a multiplicative decomposition of the deformation gradient. Strain measured relative to the zero stress state is termed the effective strain, while the classical strain associated with being at the local zero stress state is referred to as the residual strain (Cook, 1995).

Plastic tissue deformation associated with growth and cellular remodelling leads to changes in the zero stress state. Since the effective strain is measured relative to the zero stress state, these changes can be incorporated into how the effective strain develops. We assume the current state is everywhere a small elastic deformation from the local zero stress state. This enables us to consider linear elasticity based on the effective strain. In turn, our formulation for effective strain incorporates many morphological aspects of tissue repair, such as cellular remodelling of collagen fibres and the growth of new tissue. Thus, we develop a morphoelastic representation of wound repair as it can capture both the growth and mechanical considerations involved in tissue repair.

Cook (1995) uses these ideas to develop a preliminary morphoelastic model of wound closure. He assumes symmetry about the wound centre at $x = 0$, and considers two compartments: one on $0 < x < L$, which corresponds to the wound space and a second on $L < x < \alpha$, which represents the undamaged tissue (see Figure 1). In this work, $L$ is the location of the wound boundary and an increase in $L$ indicates an increase in wound size (or retraction) while a decrease in $L$ indicates wound contraction. We note that $x = \alpha$ represents an undisturbed point far from the wound and that Cook considers a value of $\alpha = 1$.

This formulation allowed Cook to consider each time-varying species in two

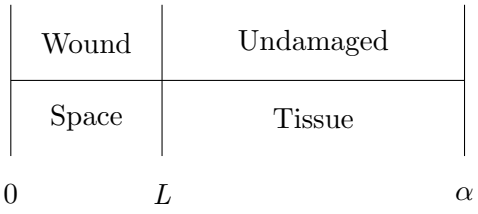


Figure 1: Wound compartment diagram.

forms: one inside the wound and another outside. Cook thus simplified his full model to one that contained only time derivatives. Since the full model included advection, this ODE approach required a representation of the spatial derivative of the velocity; Cook used the approximation

$$\frac{\partial v}{\partial x} = \begin{cases} \frac{1}{L}\frac{dL}{dt} & 0 < x < L, \\ \frac{-1}{L-\alpha}\frac{dL}{dt} & L < x < \alpha. \end{cases}$$

Combining these ideas, Cook developed the following 1D non-dimensional model of wound closure:

$$\begin{aligned} \frac{dn}{dt} &= n(1-n) - \frac{n}{L}\frac{dL}{dt}, & \frac{dz}{dt} &= \frac{\kappa q(s) n \epsilon}{s}, \\ \frac{ds}{dt} &= \kappa n(1-s) - \frac{s}{L}\frac{dL}{dt}, & \frac{dS}{dt} &= \frac{S}{1-L}\frac{dL}{dt}, \\ SE &= s\epsilon + \tau(n), & \tau(n) &= \tau_0 n(1-n)^\theta, \\ \epsilon &= \frac{L-L_0}{L} - z, & E &= \frac{L-L_0}{L-1}, \end{aligned}$$

$$q(s) = \begin{cases} 1 - \frac{s}{\beta} & \text{if} \quad s < \beta, \\ 0 & \text{if} \quad s > \beta. \end{cases}$$

Here $n$ is the fibroblast density, $s$ and $S$ are the collagen densities inside and outside the wound respectively, $\epsilon$ and $E$ are the effective strains inside and outside the lesion, $z$ is the residual strain, $\tau$ is the cell traction, $\kappa$ is the production rate of collagen, $2L_0$ is the initial wound size, $\tau_0$ is a parameter characterising the cell traction, $\theta$ is a parameter that modifies the logistic form adopted for the cell traction dependence on fibroblast density, $q(s)$

represents the proportion of fibres laid down in a relaxed state and $\beta$ is the threshold value of the residual strain above which alterations to the residual strain are negligible.

While Cook (1995) was able to describe permanent wound contraction with his model, a feature not observed in any of the previous models, there are several shortcomings, which we now describe.

Despite previous research by Tranquillo and Murray (1992) concluding that an inflammatory mediator is essential in wound repair, Cook (1995) neglects all chemical effects. In order to effect wound contraction, Cook instead assumes that the cell traction stress is biphasic. In contrast, Tamariz and Grinnell's (2002) experiments suggest that tractional stress is a monotonically increasing function of cell density, consistent with previous models of dermal repair such as those of Tranquillo and Murray (1992) and Olsen et al. (1995). A further problem with Cook's formulation is that it leads to a situation where there is no tension in the healthy skin or the healed wound; this is unrealistic (Reihsner et al., 1995).

Cook also models the effective strain explicitly. He assumes that it is governed by the movement of the wound boundary and, inside the wound, the residual strain. While Cook allows the residual strain to evolve by incorporating the effect of cells laying down new fibres, he ignores the action of cells actively remodelling the collagen matrix. However, in fibroblast populated collagen lattice experiments by Grinnell et al. (2003), it was found that significant permanent contraction occurs as a result of fibroblasts physically remodelling the lattice. We incorporate a new representation of the evolution of effective strain that includes these effects.

Finally, Cook neglects the synthesis of collagen in the unwounded region. Consequently, the steady state value of the collagen density outside the

wound is history-dependent. Hence, the collagen density inside the wound tends to healed levels but the collagen density outside the wound may not.

In the proposed mechanochemical wound repair model, we have addressed these issues and also extended Cook's model to include the presence of myofibroblasts and the effects of TGF$\beta$.

## 3. Proposed Mathematical Model

### *3.1. Two-Compartment Model of Wound Repair*

Following Cook (1995), we consider a two-compartment model for wound repair. We assume symmetry about the wound centre at $x = 0$ and take $x = L(t)$ to represent the time-dependent wound boundary, with $0 < x < L$ corresponding to one half of the wound space. We also assume that there is a fixed point, $x = \alpha$, that is sufficiently far from the wound space that the tissue is undisturbed there. In our model, $L < x < \alpha$ therefore corresponds to the unwounded dermis. We also note that the proliferative stage occurs over approximately a one month period (Enoch and Leaper, 2007) and so we measure time, $t$, in days.

Our model examines the interactions between cells, TGF$\beta$, ECM and wound mechanics. We consider eight dependent variables: the fibroblast density inside and outside the wound ($n$ and $N$ respectively), the myofibroblast density in the wound ($m$), the TGF$\beta$ concentration within the wound ($\beta$), the ECM density within and without the wound ($s$ and $S$, respectively), the effective strain within and without the wound ($e$ and $E$, respectively), and the location of the wound boundary ($L$).

Fibroblasts are assumed to undergo logistic growth, to transform into myofibroblasts in response to mechanical stimuli and to advect with the moving

ECM. It is known that fibroblasts migrate into the wound space from the surrounding dermis and we model this with a simple form: the recruitment of fibroblasts to the wound is taken to be proportional to the difference between the fibroblast density in the undamaged tissue and the density in the wound. Hence, the fibroblast equation takes the form

$$\frac{dn}{dt} = gn\left(1 - \frac{n}{\hat{N}}\right) + \frac{R(N-n)}{L} - rK\beta en - \frac{n}{L}\frac{dL}{dt}, \tag{1}$$

$$N(t) = \hat{N}, \tag{2}$$

where $g$ is the intrinsic growth rate of fibroblasts, $\hat{N}$ represents the unwounded density of fibroblasts, $R$ represents the rate at which cells migrate into the wound from the unwounded dermis, $r$ characterises the activation rate of fibroblasts to myofibroblasts, and $K$ is the elastic modulus of the dermis. Assuming tissue stiffness to be proportional to collagen density, we find that $K = Ys$, where $Y$ is a constant of proportionality.

The activation term, $rK\beta en$, has been chosen since fibroblasts are activated to myofibroblasts by the presence of TGF$\beta$ ($\beta$) and tensile stress. It should be noted that elastic stress ($Ke$) is used, rather than traction stress or total stress. This can be justified by noting that the traction stress is in fact a body force due to the action of cells. Moreover, a simple comparison of the elastic stress and traction stress profiles in the Tranquillo and Murray (1992) model makes it clear that elastic stress is the most appropriate for governing the activation of fibroblasts. The elastic stress monotonically decreases with distance away from the wound centre while traction monotonically increases. If the modulation of fibroblasts to myofibroblasts were dependent on cell traction, the monotone increase in stress would mean that the highest rate of differentiation of fibroblasts to myofibroblasts would happen outside the wound. However, using the elastic stress leads to the sensible result where activation is highest in the wound. This behaviour is consistent with the observation by Hinz et al. (2001) that myofibroblast differentiation

slows, or is even arrested, upon release of tension from splinted wounds. As the wound contracts, the elastic stress decreases and the rate of the myofibroblast differentiation also slows. This phenomenon is observed regardless of the magnitude of the initial cell traction outside the wound space.

As mentioned above, myofibroblasts are assumed to be present only within the wound space and the only source of myofibroblasts is taken to be the activation of fibroblasts. Myofibroblasts are assumed not to transform back to fibroblasts, instead undergoing natural cell death (apoptosis) (Moulin et al., 2004). In addition, these cells are advected as the ECM moves. Hence, the governing equation for the myofibroblast density is

$$\frac{dm}{dt} = rK\beta en - am - \frac{m}{L}\frac{dL}{dt}, \tag{3}$$

where $a$ characterises the rate of myofibroblast apoptosis.

Fibroblasts migrate into the wound space 2-4 days post-wounding (Enoch and Leaper, 2007) and experimental results by Yang et al. (1999) show that there is a large concentration of TGF$\beta$ in the wound space at around this time, which then decays approximately exponentially. In our model, where $t = 0$ represents day 2 post-wounding, we therefore assume that TGF$\beta$ can be modelled by an exponential decay function of the form

$$\beta(t) = \beta_0 \exp\left(-bt\right), \tag{4}$$

where $\beta_0$ is the initial concentration of TGF$\beta$ and $b$ is the natural decay rate.

The ECM is synthesized by both the fibroblasts and myofibroblasts, with production ceasing once unwounded levels are obtained. Both the ECM inside the wound and the ECM outside the lesion undergo advection as the wound retracts and contracts. Based on these assumptions, the governing

equations for ECM density are

$$\frac{ds}{dt} = k_1(n + \eta m) - k_2(n + \delta m)s - \frac{s}{L}\frac{dL}{dt}, \tag{5}$$

$$\frac{dS}{dt} = k_1 N - k_2 NS + \frac{S}{\alpha - L}\frac{dL}{dt}, \tag{6}$$

where $k_1$ and $k_2$ are the synthesis and degradation rates of ECM by fibroblasts respectively, and $\eta$ and $\delta$ are the synthesis and degradation rates of ECM by myofibroblasts relative to fibroblasts.

Strain in the ECM develops as cells rearrange the matrix, generating tension in the fibres, and is reduced when new fibres are laid down in a relaxed state. Advection also affects the local strain, with the effect of tissue elasticity represented in the $(1/L)dL/dt$ term. We consider a form of the effective strain based upon Hall's (2009) repair description, obtaining the following governing equations for strain inside and outside the wound:

$$\frac{de}{dt} = k_\zeta s(n + \pi_\zeta m) - \frac{k_\rho(n + \pi_\rho m)e}{s} + \frac{(1 - e)}{L}\frac{dL}{dt}, \tag{7}$$

$$\frac{dE}{dt} = k_\zeta NS - \frac{k_\rho NE}{S} - \frac{(1 - E)}{\alpha - L}\frac{dL}{dt}, \tag{8}$$

where $k_\zeta$ is the rate at which fibroblasts cause permanent contraction of the ECM, $\pi_\zeta$ represents the rate of permanent contraction due to myofibroblasts relative to fibroblasts, $k_\rho$ is the rate of matrix turnover as a result of replacing stressed fibres with unstressed fibres and $\pi_\rho$ represents the remodelling achieved by myofibroblasts relative to that of fibroblasts. Here $k_\zeta$, $k_\rho$, $\pi_\zeta$, $\pi_\rho$ are all constants.

It is assumed that there are no body forces apart from those due to cell traction. Consequently, the tissue forces (due to elastic and cell traction stress) inside and outside the wound must balance, leading to

$$Yse + \tau(n + \zeta m)s = YSE + \tau NS, \tag{9}$$

where $\tau$ is a constant measuring the fibroblast traction and $\zeta$ represents the strength of myofibroblasts relative to fibroblasts. This formulation also

assumes an abrupt interface between the wound and unwounded dermis. In an acute wound this interface is gradual. However, since the width of this interface is typically much smaller than the wound width, this represents a reasonable assumption. We note that in Cook's model the cell traction term is independent of collagen density; here, we take it to be directly proportional to $s$, in line with Tranquillo and Murray (1992). From (9), the governing equation for the wound boundary

$$\begin{aligned}\frac{dL}{dt} = &\frac{Y\left\{\kappa\left[E(1-S)-(n+\eta m)(1-s)e\right]+k_\zeta\left[S^2-(n+\pi m)\,s^2\right]\right\}}{\frac{s}{L}\left\{Y(1-2e)-2\tau(n+\zeta m)\right\}+\frac{S}{\alpha-L}\left\{Y(1-2E)-\tau\right\}}\\ &\frac{-Yk_\rho\left[E-(n+\eta m)\,e\right]+\tau\kappa\left[(1-S)-(n+\eta m)(1-s)(n+\zeta m)\right]}{\frac{s}{L}\left\{Y(1-2e)-2\tau(n+\zeta m)\right\}+\frac{S}{\alpha-L}\left\{Y(1-2E)-\tau\right\}}\\ &\frac{+\tau\left\{rYs^2en\beta(1-\zeta)+\zeta asm-s(1-n)\,(n+R/L)\right\}}{\frac{s}{L}\left\{Y(1-2e)-2\tau(n+\zeta m)\right\}+\frac{S}{\alpha-L}\left\{Y(1-2E)-\tau\right\}}\end{aligned}$$

is obtained by differentiating (9) with respect to time, substituting in equations (1)-(8), and rearranging for $dL/dt$.

The system is non-dimensionalised (see Appendix B), and from this point on we consider the following non-dimensional equations, dropping bars for convenience:

$$\frac{dn}{dt} = n\,(1-n) + \frac{R(1-n)}{L} - rY\beta sen - \frac{n}{L}\frac{dL}{dt}, \tag{10}$$

$$\frac{dm}{dt} = rY\beta sen - am - \frac{m}{L}\frac{dL}{dt}, \tag{11}$$

$$\beta(t) = \exp\left(-bt\right), \tag{12}$$

$$\frac{ds}{dt} = \kappa(n+\eta m)(1-s) - \frac{s}{L}\frac{dL}{dt}, \tag{13}$$

$$\frac{dS}{dt} = \kappa(1-S) + \frac{S}{1-L}\frac{dL}{dt}, \tag{14}$$

$$\frac{de}{dt} = k_\zeta s(n+\pi m) - \frac{k_\rho(n+\eta m)e}{s} + \frac{(1-e)}{L}\frac{dL}{dt}, \tag{15}$$

$$\frac{dE}{dt} = k_\zeta S - \frac{k_\rho E}{S} - \frac{(1-E)}{1-L}\frac{dL}{dt}, \tag{16}$$

$$YSE + \tau S = Yse + \tau(n+\zeta m)s. \tag{17}$$

Since $N(t) \equiv 1$, we no longer consider the fibroblast density outside the

wound space. Note, the problem is scaled so that one unit of time represents approximately one day.

Recall that we are modelling the second stage of wound healing, the proliferative phase. We assume that, initially, the scaled ECM density and the effective strain outside the wound space are given by

$$S(0) = 1 \quad \text{and} \quad E(0) = \frac{k_\zeta}{k_\rho},$$

their unwounded values. It is assumed that the wound is small and hence there is a very small population of fibroblasts in the wound initially. Additionally, we assume that there is a small amount of collagen already within the wound space. Based on these assumptions we use the initial conditions

$$L(0) = 0.1, \quad n(0) = 0.001 \quad \text{and} \quad s(0) = 0.25.$$

The strain inside the wound, $e$, must satisfy the force balance equation, (17), thus

$$e(0) = \frac{k_\zeta}{k_\rho s(0)} + \frac{\tau}{Y s(0)} - \frac{\tau n(0)}{Y}.$$

With these initial conditions, the full dimensionless system of (10)-(17) can be solved using MATLAB's inbuilt ordinary differential equation routine, *ode45*.

### *3.2. Parameter Estimation*

One complication common to almost all mathematical representations of biological systems is that it is usually impossible to determine the values of all the parameters directly from experimental evidence. In some cases, an appropriate value can be estimated based on experimental results or a plausible range can be determined; nonetheless, some parameters may need to be estimated from numerical simulations so that the predictions

are physically realistic. Clearly, assigning parameters values is a nontrivial process.

In Table 1 we present the parameters we used in our model; this table also includes a description of whether the value was known, calculated or estimated and, where appropriate, references are provided. Fortuitously, the sensitivity analysis in Section 4 shows our model to be quite robust to significant variations in a number of parameter values. This means that we can have some confidence that the solutions obtained with these parameter values is indicative of the solution trajectory for physiologically correct parameter values.

In the morphoelastic representation of tissue dynamics that we use, we assume that the zero stress state is close to the current state. This implies that the effective strain is small (i.e. $e \ll 1$) and enables us to assume linear elasticity. Given that the steady state of the effective strain in healthy skin is $k_\zeta/k_\rho$, this indicates that $k_\zeta \ll k_\rho$. With this in mind, we choose $k_\rho$ and $k_\zeta$ such that $k_\zeta/k_\rho$ is $O(10^{-2})$.

A wide range of values are reported in the present literature for the magnitude of traction forces exhibited by human dermal fibroblasts; estimates range from 0.1nN/cell (Eastwood et al., 1994, 1996, 1998; Campbell, 2002; Wrobel et al., 2002; Shreiber et al., 2003) to 2.65$\mu$N/cell (Delvoye et al., 1991; Fray et al., 1998). There is a number of possible reasons for this apparent discrepancy. Firstly, there is a lot of variation in the matrix material upon which the cells are seeded. While fibroblast populated collagen gels appear to be the most widely used, 3-D bio-artificial hydrogels (Zahalak et al., 2000), GAG-collagen scaffolds (Freyman et al., 2001), elastomers (Wrobel et al., 2002) and other 3-D constructs (Harley et al., 2007) have also been employed. Additionally, different experiments involve matrices of different stiffnesses with elastic moduli ranging from 40Pa to 70GPa (Freyman

| Non-Dimensional Parameter | Range | Reference |
|---|---|---|
| $R$, Ingress of fibroblasts | $R \approx 0.04$ | Sillman et al. (2003) |
| $r$, Fibroblast activation to myofibroblasts | $r \approx 0.22$ | Desmouliere et al. (1993) |
| $a$, Myofibroblast apoptosis | $0.096 < a < 0.24$ | Moulin et al. (2004) |
| $b$, TGF$\beta$ decay | $b \approx 0.426$ | Est. from Yang et al. (1999) |
| $\kappa$, Collagen production | $0.1 - 1$ | TW |
| $\eta$, Relative collagen production by myofibroblasts | 2 | Moulin et al. (1998), Olsen et al. (1995) |
| $k_\zeta$, Contractile strain produced by fibroblasts | $0.002 < k_\zeta < 0.02$ | TW |
| $k_\rho$, Matrix turnover by fibroblasts | $0.2 < k_\rho < 2$ | TW |
| $\pi$, Myofibroblast to fibroblast contractile strain generation | 15 | TW |
| $Y$, Elastic modulus | $10 < Y < 300$ | Silver et al. (2001), Genzer and Groenewold (2006) |
| $\tau$, Fibroblast cell traction | $1 < \tau < 3$ | Fray et al. (1998), Wrobel et al. (2002) |
| $\zeta$, Myofibroblast to fibroblast cell traction | $\zeta \approx 5$ | Olsen et al. (1995) |
| $n_0$, Initial fibroblast density | 0.001 | Cook (1995) |
| $s_0$, Initial collagen density | 0.25 | TW |
| $L_0$, Initial wound boundary | 0.1 | Cook (1995) |

Table 1: Table of parameters. Unless otherwise specified, these parameters are used for all simulations. TW refers to estimations made during this work. For determination of the dimensional parameter values see Appendix Appendix B.

et al., 2001, 2002; Campbell, 2002). None of these experiments considered a modulus between $0.1 - 0.7$MPa, the approximate stiffness of human dermal tissue (Diridollou et al., 2000; Silver et al., 2001; Khatyr et al., 2004; Genzer and Groenewold, 2006; Ahlfors and Billiar, 2007; Kucharova et al., 2007), although it is possible to manufacture collagen gels that possess an elastic modulus in the appropriate range (Chapuis and Agache, 1992; Ahlfors and Billiar, 2007). As cell traction strength is thought to vary significantly with tissue stiffness, the failure of experimental research to adequately control for tissue stiffness might account for the large variation in measured tissue stiffnesses. Moreover, the failure to use lattices of stiffness similar to that of the skin means that what results have been obtained may not be physiologically relevant.

Moreover, there is no consistency in the method used to determine the cell traction force. Current methods include studies of free-floating fibroblast-populated collagen lattices (Li and Wang, 2009), the use of cellular force monitors (Freyman et al., 2002), micropost force sensor arrays (Li and Wang, 2009), and cell traction force microscopy (Fray et al., 1998; Li and Wang, 2009). These different techniques seem to yield inconsistent measurements of the cell traction force and there is a need for further work to harmonise the various experimental approaches.

Also, it is possible that the variation in cell traction estimates is associated with mixed populations of fibroblasts and myofibroblasts and with the effects of fibroblasts differentiating into myofibroblasts. Myofibroblasts are known to function in a manner similar to smooth muscle cells, and cell traction values of $1\mu$N/cell are close to those of smooth muscle cells at $1.5\mu$N/cell (Wakatsuki et al., 2000). Hence, cell traction values around 1nN/cell may correspond to the force generated by fibroblasts, while values near $1\mu$N/cell may be associated with myofibroblasts.

We have also reviewed the non-dimensional values of the traction force used by previous biomathematicians who have modelled dermal repair. Even amongst these papers there are discrepancies. There are two clusters of values used by researchers; some authors used cell traction parameters in the range $0.02 - 0.05$ (Olsen et al., 1995; Ferrenq et al., 1997; Tranqui and Tracqui, 2000) while others took traction to be in the range $0.5 - 2$ (Tranquillo and Murray, 1992; Cook, 1995; Tracqui et al., 1995; Tranqui and Tracqui, 2000; Ramtani et al., 2002; Ramtani, 2004). It is possible that this discrepancy is partly due to the different non-dimensionalisations used by the authors. The cell traction parameter depends on the scaling of cell density, which varies significantly in different papers from $O(10^3)$ to $O(10^6)$ (Olsen et al., 1996; Ferrenq et al., 1997). This may account for the order of magnitude variation in the non-dimensionalised cell traction parameter.

The previous model by Cook (1995) (on which this work is based) used a non-dimensional cell traction value of 2. Therefore, it is reasonable to assume that the non-dimensional value of cell traction in this work should be of $O(1)$. Consideration of the scaling then implies that the cell traction force is approximately $2\mu$N/cell, consistent with Kolodney and Wysolmerski (1992), Fray et al. (1998), Wakatsuki et al. (2000), Wrobel et al. (2002) and Wagenseil and Okamoto (2007).

## 4. Results

Following Cook (1995), we consider the effect of varying particular parameter values on the system. The significant results are summarised in Table 2.

| $r$ | $a$ | $b$ | $\kappa$ | $k_\zeta$ | $\pi$ | $k_\rho$ | $\tau$ | $s_0$ | $\frac{L_m}{L_0}$ | $\frac{L_f}{L_0}$ | Comment |
|---|---|---|---|---|---|---|---|---|---|---|---|
| 0.22 | 0.2 | 0.426 | 0.27 | 0.0054 | 15 | 0.54 | 2 | 0.25 | 1.035 | 0.917 | Base Case |
| **0.44** | 0.2 | 0.426 | 0.27 | 0.0054 | 15 | 0.54 | 2 | 0.25 | 1.016 | *0.852* | Increase fibroblast activation |
| 0.22 | **0.1** | 0.426 | 0.27 | 0.0054 | 15 | 0.54 | 2 | 0.25 | 1.032 | *0.752* | Increase myofibroblast lifespan |
| 0.22 | 0.2 | **0.213** | 0.27 | 0.0054 | 15 | 0.54 | 2 | 0.25 | 1.027 | *0.851* | Slower TGF$\beta$ decay or longer inflammatory response |
| 0.22 | 0.2 | 0.426 | **0.54** | 0.0054 | 15 | 0.54 | 2 | 0.25 | 1.000 | *0.845* | Increased collagen production |
| 0.22 | 0.2 | 0.426 | 0.27 | **0.0108** | 15 | 0.54 | 2 | 0.25 | 1.060 | *0.753* | Greater contractile strain |
| 0.22 | 0.2 | 0.426 | 0.27 | 0.0054 | 15 | 1.08 | 2 | 0.25 | 1.181 | `1.077` | Increased remodelling |
| 0.22 | 0.2 | 0.426 | 0.27 | **0.0108** | 15 | **1.08** | 2 | 0.25 | 1.239 | *1.004* | Increased contractile strain and collagen remodelling |
| 0.22 | 0.2 | 0.426 | 0.27 | 0.0054 | **30** | 0.54 | 2 | 0.25 | 1.030 | 0.822 | Increased myofibroblast strain production |
| 0.22 | 0.2 | 0.426 | 0.27 | 0.0054 | 15 | 0.54 | **1** | 0.25 | 1.037 | `0.965` | Decreased cell traction |
| 0.22 | 0.2 | 0.426 | 0.27 | 0.0054 | 15 | 0.54 | 2 | **0.1** | 1.222 | `1.127` | Less collagen in wound initially |

Table 2: Varying parameters in a 1-D wound. **Bold** numbers represent the actual parameter varied, those that are in *italics* or `typewriter text` indicate a significant decrease or increase in wound size when compared to the base set. Also, $L_m$ is the maximum retraction of the wound boundary, and $L_f$ is the final position of the wound boundary. Only results for which there was greater than a 5% difference in final wound position relative to the base case are shown. The remaining parameters had base values of $R = 0.04$, $\eta = 2$, $Y = 71.3$, $\zeta = 5$, $n_0 = 0.001$ and $L_0 = 0.1$.

*4.1. Base Results*

In the base system (illustrated in Figure 2) we see that the fibroblast density, $n$, increases rapidly over the first week of wound repair, essentially reaching near-healed densities around day 5. Myofibroblasts undergo the greatest activation early on, achieving a maximum density on day 3, after which the myofibroblast density, $m$, decreases due to a reduction in the number of fibroblasts activated to become myofibroblasts. This decrease is primarily associated with the decay of TGF$\beta$; as $\beta$ decreases, there is a corresponding reduction in the activation of fibroblasts to myofibroblasts.

The collagen density inside the wound, $s$, follows the fibroblast profile with a lag, attaining close to a healed density by day 12. Changes in the collagen density outside the wound, $S$, are entirely mediated by the advection of the wound boundary. Thus, $S$ increases during the retraction phase, decreases while the wound contracts and finally tends towards healed levels as the damaged dermis is repaired.

Initially, the wound boundary, $L$, retracts. This expansion in wound size is due to the unbalanced stressed acting on the wound boundary. As Watts (1960) comments, "contraction is essentially a cellular process affecting the edge of the wound." Early in the healing process, there is greater cell traction stress outside the wound than within it. As such, the wound boundary is pulled open. Typically, retraction occurs over the first 2 days of wound repair (Billingham and Medawar, 1955; McGrath and Emery, 1985), and we predict maximum retraction to occur just following two days of repair. As the wound space is repopulated with fibroblasts and as fibroblasts are transformed into myofibroblasts, cell traction stress within the wound increases beyond that of the surrounding tissue, and wound contraction results.

This ensuing contractile phase is approximately exponential in nature. The

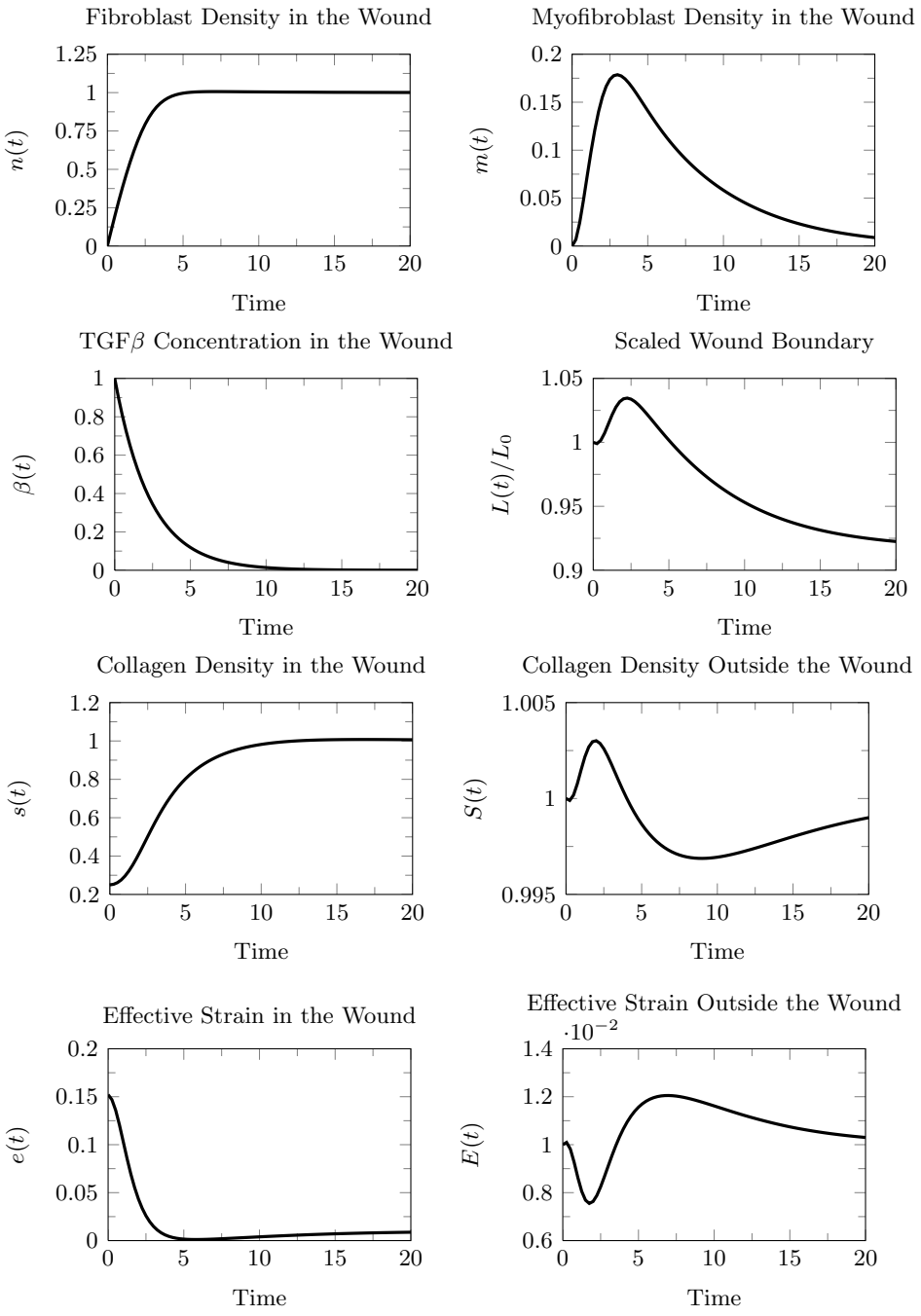


Figure 2: Dermal repair profiles predicted by the model. Parameter values were $\kappa = 0.27$, $\tau = 2$, $k_\zeta = 0.0054$, $k_\rho = 0.54$, $Y = 71.3$, $R = 0.04$, $r = 0.22$, $a = 0.2$, $\zeta = 5$, $\pi = 15$, $\eta = 2$ and $b = 0.426$.

contractile phase is highly dependent on the presence of myofibroblasts. However, fibroblast activation decreases as the wound heals; fewer myofibroblasts are generated and apoptosis dominates, reducing the density of myofibroblasts. This causes contraction of the wound to decrease also, reaching a plateau stage where further contraction is negligible. By this stage, it is observed that approximately 10% of wound closure has been effected by wound contraction, which is consistent with previous predictions of human dermal wound repair (Murray, 2003).

### *4.2. Varying the activation rate of fibroblasts, r*

As expected, increasing (decreasing) the activation rate of fibroblasts to myofibroblasts significantly increases (decreases) the myofibroblast density (see Figure 3), while having only a limited effect on fibroblast density. If the activation rate is very small, there are few myofibroblasts. As a result, the total traction stress associated with the cells is significantly weaker and the wound boundary may retract and stay retracted (instead of contracting). In contrast, if the activation rate is quite high, there may be no initial retraction. Thus, the system exhibits contraction only and, due to the increased myofibroblast density, the contraction of the wound boundary is significantly increased. Variations in the remainder of the system are essentially due to advection.

### *4.3. Varying the rate of myofibroblast apoptosis, a*

When the apoptotic rate of myofibroblasts is increased so that myofibroblasts die out rapidly, there is only a marginal difference in the fibroblast profile (see Figure 4).

In the case where myofibroblast apoptosis is small, the effective strain inside the wound is reduced, decreasing the activation rate and causing the

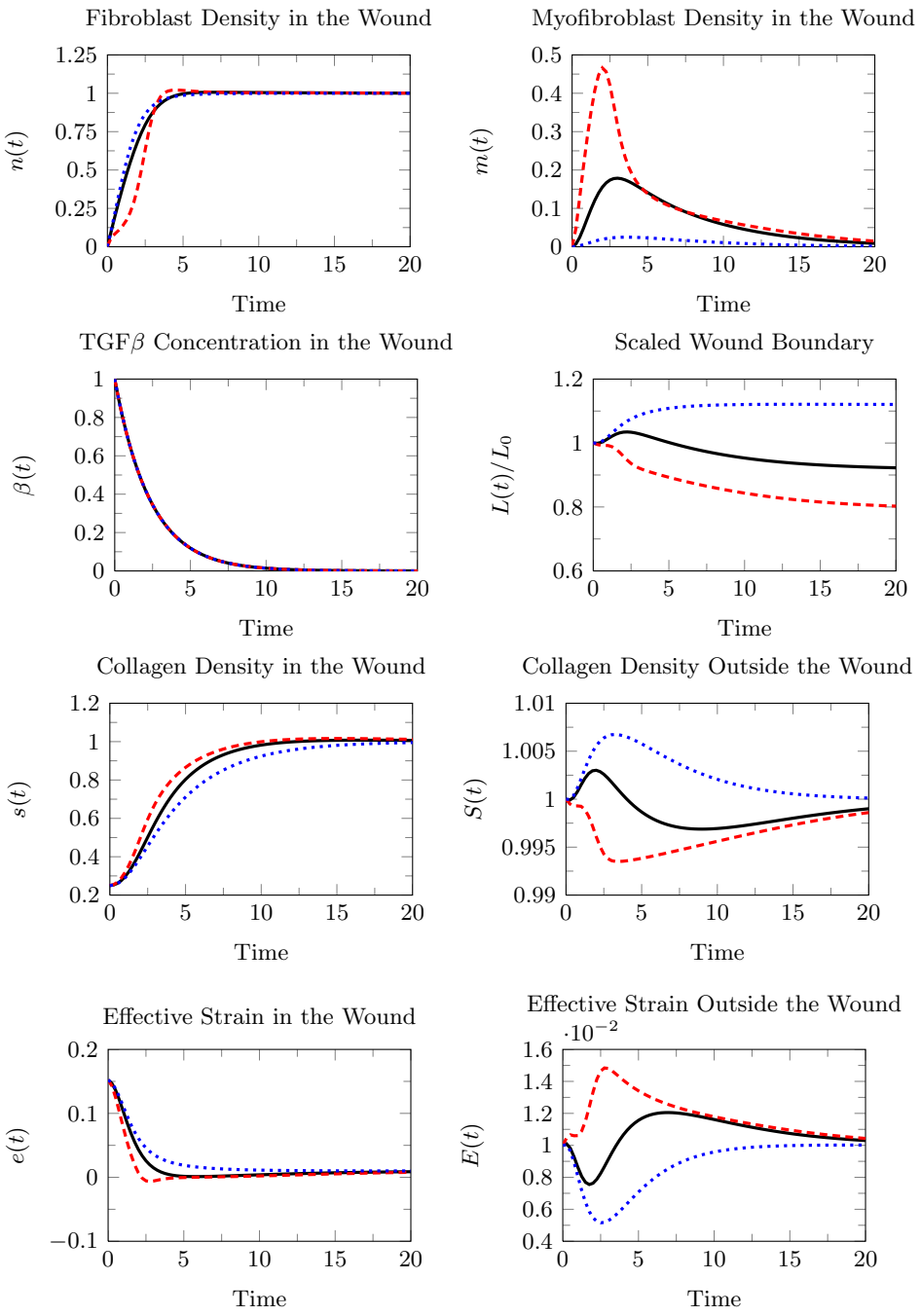


Figure 3: The fibroblast activation rate was varied by multiplying or dividing the base activation rate of 0.22 by 10, so that the activation rates considered were $r = 2.2$ (- -), $r = 0.22$ (-) and $r = 0.022$ (..). The other parameter values were $\kappa = 0.27$, $\tau = 2$, $k_\zeta = 0.0054$, $k_\rho = 0.54$, $Y = 71.3$, $R = 0.04$, $a = 0.2$, $\zeta = 5$, $\pi = 15$, $\eta = 2$ and $b = 0.426$.

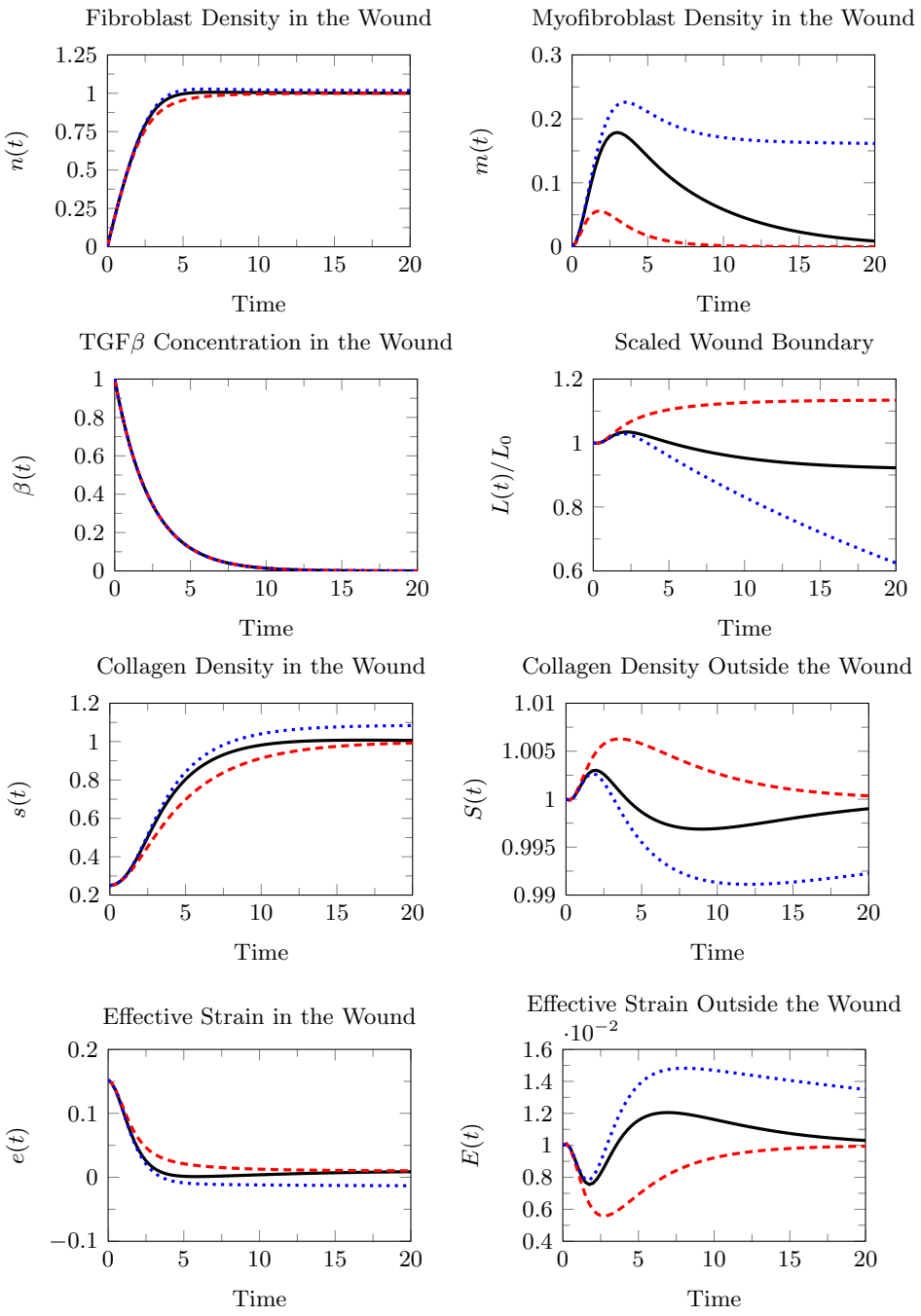


Figure 4: The rate of myofibroblast apoptosis was varied by roughly one order of magnitude from the base rate of 0.2, so that the death rates considered were $a = 2$ (- -), $a = 0.2$ (-) and $a = 0.03$ (..). The other parameter values were $\kappa = 0.27$, $\tau = 2$, $k_\zeta = 0.0054$, $k_\rho = 0.54$, $Y = 71.3$, $R = 0.04$, $r = 0.22$, $\zeta = 5$, $\pi = 15$, $\eta = 2$ and $b = 0.426$.

fibroblast density to achieve unwounded levels more quickly. While the activation rate is small in this case, the maximum myofibroblast density significantly increases with decreasing apoptotic rate since myofibroblasts persist for longer. Indeed, for sufficiently small apoptosis the myofibroblasts increase collagen density within the wound space and cause excessive wound contraction, both of which persist for some time following wound closure.

In summary, increasing (decreasing) the rate at which myofibroblasts undergo apoptosis causes the system to behave in a manner similar to when the fibroblast differentiation rate is decreased (increased). For instance, increasing the activation rate resulted in excess collagen, while decreasing the myofibroblast apoptotic rate predicted the same outcome.

### *4.4. Varying the decay rate of TGF$\beta$, b*

Decreasing the decay rate of TGF$\beta$ achieves a similar effect to reducing myofibroblast apoptosis (see Figure 5). When TGF$\beta$ persists, the activation of fibroblasts to myofibroblasts is prolonged. Consequently, myofibroblasts remain following wound closure, causing a mild increase in collagen production within the wound space as well as continued severe wound contraction. If, on the other hand, the decay rate is increased, fibroblast differentiation ceases quickly and few myofibroblasts are produced. This causes the wound boundary to retract permanently and in this case, the wound expands to cover an area approximately 120% that of the original.

### *4.5. Comparison with Experimental Data*

Currently, there is no experimental data for human full thickness wounds showing the three phases of wound boundary movement (retraction, exponential contraction and permanent contraction). Multiple studies measuring

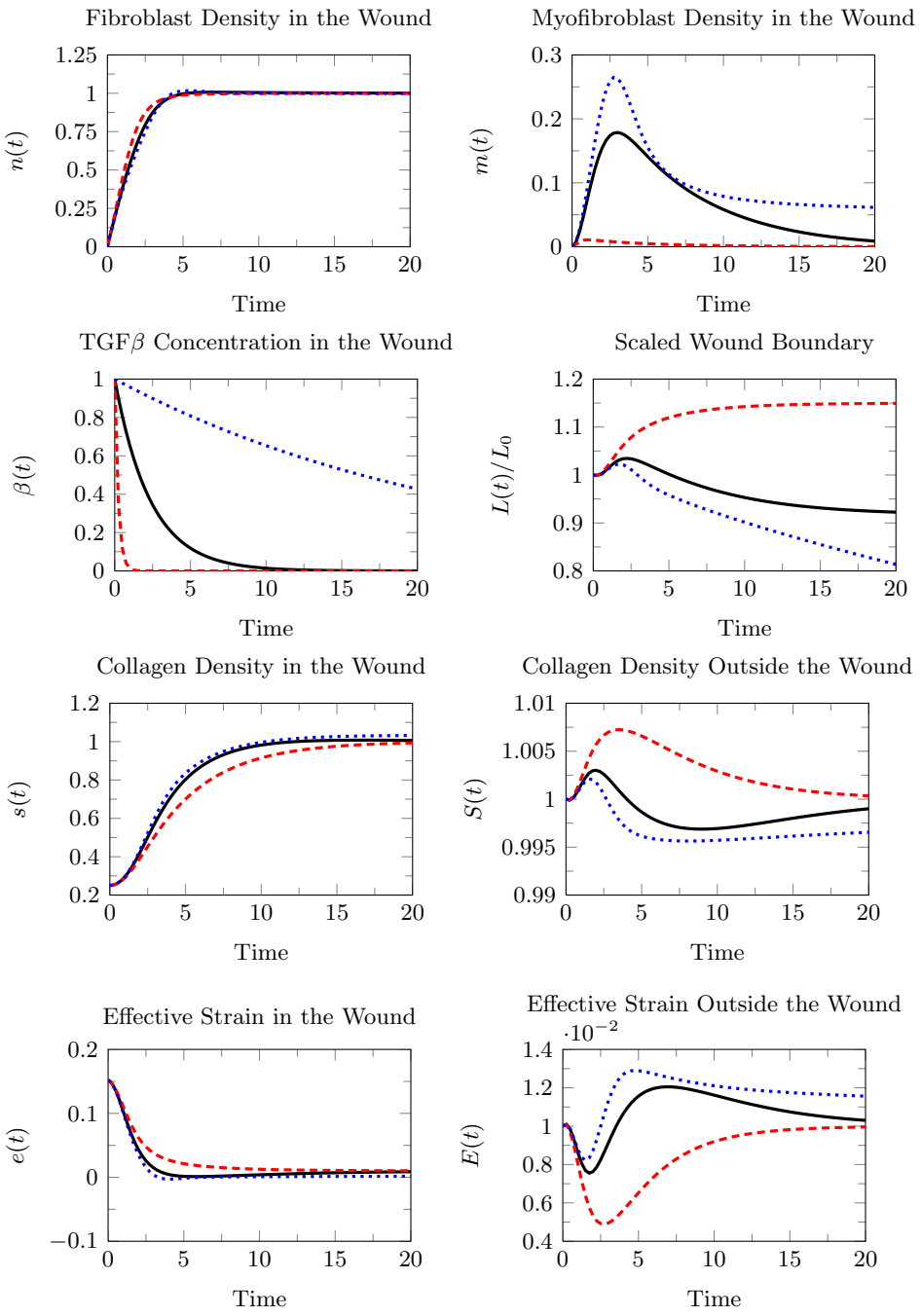


Figure 5: The decay rate of TGF$\beta$ was varied by multiplying or dividing the base decay rate of 0.1 by 10, so that the decay rates considered were $b = 4.26$ (- -), $b = 0.426$ (-) and $b = 0.0426$ (..). The other parameter values were $\kappa = 0.27$, $\tau = 2$, $k_\zeta = 0.0054$, $k_\rho = 0.54$, $Y = 71.3$, $R = 0.04$, $r = 0.22$, $a = 0.2$, $\zeta = 5$, $\pi = 15$ and $\eta = 2$.

wound contraction have been conducted (Billingham and Medawar, 1955; Billingham and Russell, 1956; Grillo et al., 1958; Watts, 1960; Luccioli et al., 1964; Kennedy and Cliff, 1979; Doillon et al., 1987). However, the results that most ably illustrate the three stages of wound movement are those obtained by McGrath and Simon (1983). Therefore, the model was tested by comparing our predictions with McGrath and Simon's (1983) experimental results of rat wound contraction. Figure 6 shows their experimental results plotted against our simulation curve.

The only alteration made to the parameter values was to the values of $k_\rho$, which reflects the proportion of collagen fibres that are laid down pre-stressed, and $k_\zeta$, the rate at which fibroblasts cause permanent strain in the lattice. In the early figures, we have used $k_\zeta = 0.0054$ and $k_\rho = 0.54$, but the McGrath-Simon data can be fitted well with the values $k_\zeta = 0.0235$ and $k_\rho = 0.81$. Hence, it appears that, in comparison with human wound healing, rat dermal repair involves greater contraction of collagen fibres relative to collagen production. This is consistent with the observation that rat wounds heal primarily by contraction while human injuries heal primarily by migration and proliferation. Indeed, rat skin contains an additional organ, the panniculus carnosus, which changes the elasticity of the skin and acts to pull the wound closed mechanically. This affects the mechanical behaviour of the skin and would need to be reflected within our model. Since the panniculus carnosus moves the substratum of the skin and effectively holds the wound closed while it heals, we expect that the presence of the panniculus carnosus should principally affect the morphoelastic properties of the skin. This is consistent with the fact that we obtain a good fit between our model and the McGrath-Simon data by modifying the parameters $k_\rho$ and $k_\zeta$, which both appear in the strain evolution equation.

From Figure 6, it appears that the time scale of retraction is different as

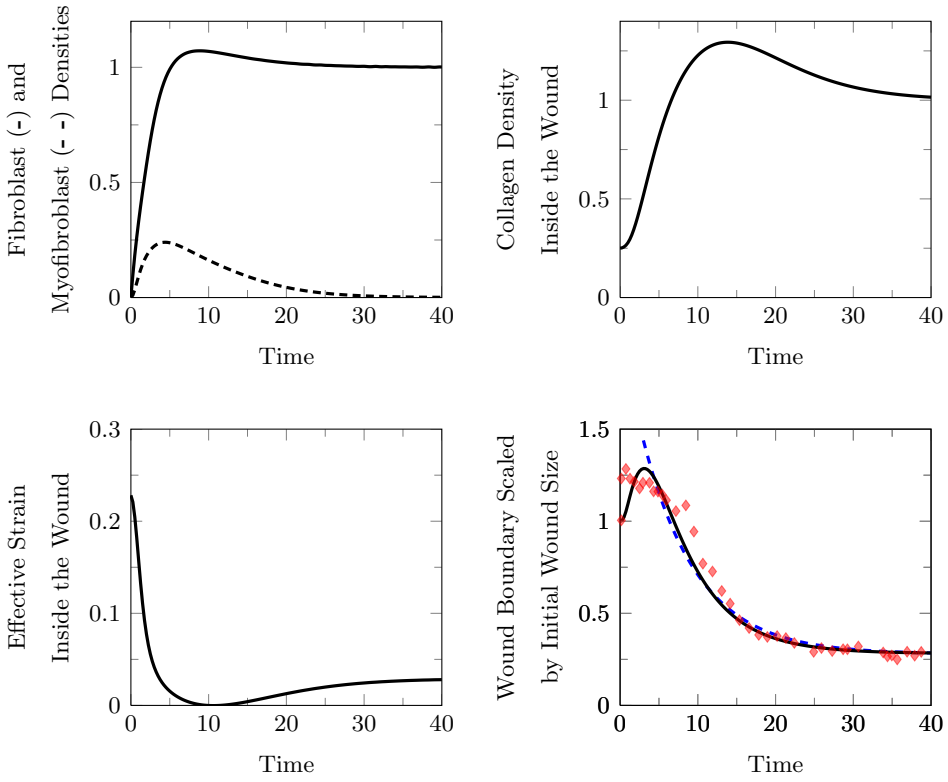


Figure 6: Comparison of our predicted curves with McGrath and Simon's (1983) experimental results for rat dermal repair. All black curves correspond to our simulated results, the red points on the wound boundary figure correspond to McGrath and Simon's experimental results, and the blue curve has been fitted to the contractile phase of our simulation to illustrate that exponential contraction is observed, with its equation given by $A(t) = 0.28 + 1.49\exp(-0.141t)$. Clearly we see that there is a large initial retraction followed by a slow permanent contraction. The fibroblasts and collagen increase to unwounded values and the TGF$\beta$ concentration tends to zero. Myofibroblasts increase while the TGF$\beta$ concentration is high, until apoptosis dominates and the myofibroblast density tends to zero. The parameter values were $\kappa = 0.27$, $\tau = 2$, $k_\zeta = 0.0235$, $k_\rho = 0.81$, $Y = 71.3$, $R = 0.04$, $r = 0.22$, $a = 0.2$, $\zeta = 5$, $\pi = 15$, $\eta = 2$ and $b = 0.426$. In order to compare dimensional and non-dimensional results we scaled time in McGrath and Simon's data by the same factor that time was non-dimensionalised by for our model; the fibroblast proliferation rate, $g$, where $g = 0.832$/day.

predicted by the model and observed in McGrath and Simon's (1983) experimental data. Rat dermal tissue is highly elastic and typically retracts fully over the first day of repair. However, wound geometry may affect the time at which maximum retraction is observed. McGrath and Simon (1983) observed small square wounds to require approximately one and a half days to retract, while circular wounds (as seen in Figure 6) retract over the first day of repair. The model predicts wound retraction to terminate on day 3. The difference is likely due to the inability to approximate values for the strain parameters $k_\rho$ and $k_\zeta$ and that in lieu of a measure for the elasticity of rat tissue, the Young's modulus for human dermis has been used.

To verify that the model predicted exponential contraction of the wound, the following exponential decay function was fitted to the contractile stage of the simulation curve,

$$A(t) = A_f + (A_0 - A_f)\exp(-kt),$$

where $A_0$ is the wound size when contraction begins and $A_f$ is the final area once contraction is completed. The constants $A_0$ and $A_f$ are both scaled with respect to $L_0$ and $k$ is the contraction rate constant. It was found that values of $A_0 = 2.05$, $A_f = 0.279$ and $k = 0.141$ generated the best approximation to the simulation curve and the approximation is shown as the dashed curve in Figure 6. This exponential function closely modelled the contractile phase of wound repair; as such we are satisified that the model predicts an exponential rate of wound contraction.

From Figure 6, we see that the model simulation appears to make a good approximation to the contraction data from McGrath and Simon (1983). To verify this, we quantitatively compare the experimental wound boundary data from McGrath and Simon (1983) with our model predictions and the exponential curve fitted to our simulation. Table 3 gives the scaled values for initial wound size, maximum retraction, one month following wounding,

and after 71 days observed by McGrath and our simulation curves. The final measurement is given at 71 days post wounding as this represents the time at which McGrath and Simon ceased recording data for rat wound contraction.

| Series | Initial | Maximum Retraction | One Month | Final (71 Days) |
|---|---|---|---|---|
| McGrath | 1.000 | 1.284 | 0.2914 | 0.3048 |
| Model | 1.000 | 1.286 | 0.2973 | 0.2817 |
| Exponential | - | 1.439 | 0.3041 | 0.2787 |

Table 3: Data from McGrath and Simon (1983) together with the corresponding predictions from our model. Wound measurements are typically carried out to one month, as such we include these measurements together with the initial wound area, maximum wound area following retraction and final wound area at 71 days.

From Table 3, we can see that our model predictions are very similar to the experimental data obtained by McGrath and Simon (1983). This confirms that good agreement is seen between the model predictions and the experimental data. The only noticable difference occurs when comparing the one month and final measurements. The wounds observed by McGrath and Simon were observed to experience late retraction. Our model however predicted a mild further contraction to occur over the same period of time. Nonetheless, the difference between this measurements is so small as to be considered negligible. Regardless, the model compares well with the experimental data. When comparing the model predictions and exponential curve, good agreement is also seen, apart from the maximum contraction. However, both from Table 3 and Figure 6 it can be seen that the exponential curve ably approximates the simulation curve.

Finally, good agreement is observed between the experimental and simulated results and so we are satisfied that the model is producing realistic results.

## 5. Discussion

We have developed a mechanochemical model of wound repair that combines a realistic representation of tissue mechanics with known cell and chemical indicatory dynamics. In particular, we consider a morphoelastic description of tissue mechanics. This gives an improved representation of strain within the system by incorporating remodelling and growth of the tissue. In addition, the activation of fibroblasts to myofibroblasts is taken to be dependent on both TGF$\beta$ *and* mechanical strain, consistent with recent experiments (Hinz, 2007; Wells and Discher, 2008). Finally, we incorporated deposition and degradation of collagen into our model and developed a force balance equation to include the contribution of myofibroblasts to cell traction.

This representation of dermal repair is capable of reproducing the contractile behaviour of acute wounds, simulating the two transient aspects of wound closure (retraction and exponential contraction) as well as the permanent reduction in wound area observed experimentally (McGrath and Simon, 1983; McGrath and Emery, 1985). This repair description is an advance on previous models of wound repair since it does not require an artificial mechanism to induce permanent wound contraction. In addition, the model has been shown to reproduce McGrath and Simon's (1983) experimental data for rat dermal repair and, using realistic parameter values, it accurately models the course of adult human dermal repair.

A parameter investigation was carried out to determine the influence of TGF$\beta$ concentration and myofibroblast density on the wound healing process. Variation of the decay rate of TGF$\beta$ was used as an indicator of the

length of the inflammatory response, with small decay rates indicating a long inflammatory response. In the case of "inflamed" wounds, a myofibroblast population is maintained after wound closure, ultimately resulting in excess contraction. For a short inflammatory response, the myofibroblast density decreases rapidly and there is in an increase in wound size.

These results suggest that TGF$\beta$ is required for wound contraction; a deficiency in TGF$\beta$ results in very few myofibroblasts and this leads to an increase in wound area. However, an excessive inflammatory response results in a heightened myofibroblast density and the possible developement of contractures.

In further simulations it was found that certain other parameter changes could lead to similar results. Indeed, the effect of a long inflammatory response could be replicated by either increasing the fibroblast activation rate or by decreasing myofibroblast apoptosis. Hence, there are different mechanisms that can initiate pathological scarring. Indeed, work by Aarabi et al. (2007) found that application of mechanical loading of murine wounds during the early proliferative stage resulted in the formation of hypertrophic scars due to down-regulated myofibroblast apoptosis. Likewise, our results suggest that an elevated myofibroblast density is key to invoking excessive contraction of wounds. Indeed, to verify this idea the system was extended to include stress dependence for myofibroblast apoptosis. The results, which for brevity are not included here, found that significantly more myofibroblasts were required to undergo apoptosis then when myofibroblast apoptosis is not stress dependent in order to obtain normal repair. Therefore, if a wound appears to be exhibiting severe contraction, it may be beneficial to reduce the myofibroblast density within the wound to prevent the development of a problematic contracture.

A reasonable fit to McGrath and Simon (1983)'s experimental data was

obtained by adjusting just two parameters: $k_\rho$, the proportion of fibres laid down that are prestressed, and $k_\zeta$, the rate of morphoelastic remodelling of the collagen network by cells acting on collagen fibres. The parameter $k_\rho$ was increased from 0.54 to 0.81, representing an increased percentage of prestressed fibres in the healing wound. The parameter $k_\zeta$ was also increased from 0.0054 to 0.0235, representing a four-fold increase in the contractile strain produced by cells. This indicates a difference between the repair responses of human and murine wounds. The significant increase in the value of $k_\zeta$ from human to murine repair indicates that murine wounds achieve closure with significantly more contraction that human dermal wounds (a fact supported by experimental evidence). Furthermore, the high $k_\rho$ value compared with the $k_\zeta$ value in human repair indicates that repair is primarily attributable to synthesis of collagen and cellular proliferation. Thus, our model suggests human wounds heal mainly by infilling, which is consistent with experimental observations.

Significant difficulties were encountered when obtaining reliable experimental estimates of some parameter values, especially parameters pertaining to mechanics. As noted above, the variability in experimental values for fibroblast traction reflects the wide range of matrix polymers, matrix elasticities and measurement techniques used in the experiments. We estimated parameter values by fitting to the qualitative details of human wound healing. However, the fact that it is possible to synthesise collagen lattices with similar mechanical properties to the skin suggests that it may be possible to develop better estimates based on experiments.

The model could be extended in various ways. For example, the representation of the matrix present in the wound before the healing process begins could be improved. It is known that a provisional matrix composed largely of fibrin is present in the wound at the beginning of the proliferative phase.

Fibroblasts degrade this fibrin network, replacing it with collagen (Shultz et al., 2005; Enoch and Leaper, 2007). Although the current initial condition of $s(0) = 0.25$ could be thought of as representing the fibrin, we would like to model the fibrin and collagen separately, with the fibroblasts degrading the local fibrin matrix and replacing it with collagen. The contribution of the fibrin lattice towards tissue stiffness and cell traction would be included. Taken together, this would enable a smaller initial collagen concentration to be considered, which would more realistically describe the early stages of wound healing.

Another aspect of the system that could be revised is the representation of the inflammatory response and its impact on the proliferative phase of wound repair. There are a number of key chemokines released during the inflammatory response and these chemokines affect the progress of proliferation. Indeed, defective inflammation is implicated in poor healing responses such as chronic wounds and pathological scarring. Additionally, greater interaction between the cellular and chemical components would be a useful way of extending the model. For example, TGF$\beta$ is known to upregulate fibroblast proliferation and act as a chemoattractor for these cells. However, the inflammatory response itself is very complicated, with macrophages, mast cells, neutrophils and platelets all playing significant roles. Each of these cells are also primary sources of inflammatory mediators in wound repair, such as TGF$\beta$, PDGF, basic fibroblast growth factor (bFGF), platelet activating factor (PAF) and many more (Majno and Joris, 2004). A simple extension of the model would be to include an equation for a generic inflammatory cell, perhaps a leukocyte, where its behaviour is representative of the net inflammatory response of these cells. In so doing, we would also be modelling one of the primary sources of TGF$\beta$, and so the behaviour of TGF$\beta$ within the system would also be more realistic.

One inflammatory cell that is known to be directly linked to the fibrotic response is the mast cell (Majno and Joris, 2004). Mast cells are recruited early in the inflammatory process and release vast quantities of growth factors via degranulation. Amongst these is PAF, which aids the platelet cascade and the subsequent release of inflammatory mediators, and bFGF, which stimulates fibroblast proliferation and recruitement to the wound site. Hence, instead of modelling a generic inflammatory cell, a possible extension would be to explore a single aspect of inflammation and investigate its effects on the proliferative response in isolation. Only considering an extension to the inflammation model presupposes that the interaction between the inflammatory and proliferative responses in the wound is the most crucial in wound repair. This may not be true, as angiogenesis is known to be intertwined with proliferation.

Angiogenesis and proliferation occur at about the same time as fibroblasts lay down the collagen through which the endothelial cells migrate as they extend and develop the vasculature system. Indeed, supply of blood is crucial to repair as oxygen levels are thought to be critical in wound closure. Furthermore, oxygen affects the rate of recruitment of fibroblasts through the wound space, the rate at which fibroblasts differentiate into myofibroblasts and the apoptotic rate of myofibroblasts. We have shown that the role of myofibroblasts in wound repair is crucial to wound contraction. Thus, factors like oxygen concentration that affect these cells are certainly worth consideration. Therefore, the inclusion of angiogenesis in future models would be valuable to elucidate the mechanisms that lead to poor wound repair.

Finally, the model developed represents a time-only description. However, there are numerous aspects of wound repair that cannot be assessed through this representation. Wound depth is known to influence the likelihood that

a wound will develop with scar hypertrophy (Enoch and Leaper, 2007), and both wound geometry and the anisotropic distribution of forces across the wound influence wound closure and the cosmetic appearance of the resulting scar (Watts, 1960; McGrath and Simon, 1983). Indeed, other possible indicators of scar quality such as collagen fibre alignment can only be considered within a spatially-dependent framework (Ferguson and O'Kane, 2004). Hence, this model could be extended to include spatial dependence.

## 6. Acknowledgements

This research was supported under the Australian Research Council's Discovery Projects funding scheme (project number DP0878011) and by the Institute of Health and Biomedical Innovation. This publication was based on work supported in part by Award No. KUK-C1-013-04, made by King Abdullah University of Science and Technology (KAUST).

## References

S Aarabi, K.A. Bhatt, Y. Shi, J. Paterno, E.I. Chang, S.A. Loh, J.W. Holmes, M.T. Longaker, H. Yee, and G.C. Gurtner. Mechanical load initiates hypertrophic scar formation through decreased cellular apoptosis. *Journal of the Federation of American Societies for Experimental Biology*, 21:3250–3261, 2007.

J.-E.W. Ahlfors and K.L. Billiar. Biomechanical and biochemical characteristics of a human fibroblast-produced and remodeled matrix. *Biomaterials*, 28:2183–2191, 2007.

B. Alberts, D. Bray, J. Lewis, M. Raff, K. Roberts, and J.D. Watson. *The Molecular Biology of the Cell*. Garland Publ. Inc., New York, 1989.

M. Aumailley, T. Krieg, G. Razaka, P.K. Müller, and H. Bricaud. Influence of cell density on collagen biosynthesis in fibroblast cultures. *Biochemical Journal*, 206:505–510, 1982.

R.E. Billingham and P.B. Medawar. Contracture and intussusceptive growth in the healing of extensive wounds in mammalian skin. *Journal of Anatomy*, 89:114–123, 1955.

R.E. Billingham and P.S. Russell. Studies on wound healing, with special reference to the phenomenon of contracture in experimental wounds in rabbits' skin. *Annals of Surgery*, 144:961–981, 1956.

B.H. Campbell. An *in vitro* study of human fibroblast contractility and the differential effect of tgf-$\beta$1 and tgf-$\beta$3 on fibroblast contraction and collagen synthesis. Master's thesis, University of Pittsburgh, 2002.

J.E. Chapuis and P. Agache. A new technique to study the mechanical properties of collagen lattices. *Journal of Biomechanics*, 25:115–117, 1992.

J. Cook. *A mathematical model for dermal wound healing: wound contraction and scar formation.* PhD thesis, University of Washingston, 1995.

P. Delvoye, P. Wiliquet, J-L. Levêque, B.V. Nusgens, and C.M. Lapière. Measurement of mechanical forces generated by skin fibroblasts embedded in a three-dimensional collagen gel. *Journal of Investigative Dermatology*, 97:898–902, 1991.

A. Desmouliere, A. Geinoz, F. Gabbiani, and G. Gabbiani. Transforming growth factor-$\beta$1 induces $\alpha$-smooth muscle actin expression in granulation tissue myofibroblasts and in quiescent and growing cultured fibroblasts. *The Journal of Cell Biology*, 122:103–111, 1993.

S. Diridollou, D. Black, J.M. Lagarde, and Y. Gall. Sex- and site-dependent

variations in the thickness and mechanical properties of human skin *in vivo*. *International Journal of Cosmetic Science*, 22:421–435, 2000.

C.J. Doillon, R.M. Hembry, H.P. Ehrlich, and J.F. Burke. Actin filaments in normal dermis and during wound healing. *American Journal of Pathology*, 126:164–170, 1987.

M. Eastwood, D.A. McGrouther, and R.A. Brown. A culture force monitor for measurement of contraction forces generated in human dermal fibroblast cultures: evidence for cell-matrix mechanical signalling. *Biochimica et Biophysica Acta (BBA) - General Subjects*, 1201:186–192, 1994.

M. Eastwood, R. Porter, U. Khan, G. McGrouther, and R. Brown. Quantitative analysis of collagen gel contractile forces generated by dermal fibroblasts and the relationship to cell morphology. *Journal of Cellular Physiology*, 166:33–42, 1996.

M. Eastwood, D.A. McGrouther, and R.A. Brown. Fibroblast responses to mechanica forces. *Proceedings of the Institution of Mechanical Engineers, Part H: Journal of Engineering in Medicine*, 212:85–92, 1998.

B. Eckes, R. Nischt, and T. Krieg. Cell-matrix interactions in dermal repair and scarring. *Fibrogenesis and Tissue Repair*, 3, 2010.

S. Enoch and D.J. Leaper. Basic science of wound healing. *Surgery*, 26: 31–37, 2007.

S. Enoch, J.E. Grey, and K.G. Harding. Abc of wound healing: Recent advances and emerging treatments. *British Medical Journal*, 332:962–965, 2006.

R.M. Farahani and L.C. Kloth. The hypothesis of 'biophysical matrix contraction': wound contraction revisited. *International Wound Journal*, 5: 477–482, 2008.

M.W.J. Ferguson and S. O'Kane. Scar-free healing: from embryonic mechanisms to adult therapeutic intervention. *Philosophical Transactions of the Royal Society of London B*, 359:839–850, 2004.

I. Ferrenq, L. Tranqui, B. Vaihé, P.Y. Gumery, and P. Tracqui. Modelling biological gel contraction by cells: mechanocellular formulation and cell traction force quantification. *Acta Biotheretica*, 45:267–293, 1997.

T.R. Fray, J.E. Molloy, M.O. Armitage, and J.C. Sparrow. Quantification of single human dermal fibroblast contraction. *Tissue Engineering*, 4: 281–291, 1998.

T.M. Freyman, I.V. Yannas, R. Yokoo, and L.J. Gibson. Fibroblast contraction of a collagen-gag matrix. *Biomaterials*, 22:2883–2891, 2001.

T.M. Freyman, I.V. Yannas, R. Yokoo, and L.J. Gibson. Fibroblast contractile force is independent of the stiffness which resists the contraction. *Experimental Cell Research*, 272:153–162, 2002.

G. Gabbiani. The myofibroblast in wound healing and fibrocontractive diseases. *The Journal of Pathology*, 200:500–503, 2003.

J. Genzer and J. Groenewold. Soft matter with hard skin: From skin wrinkles to templating and material characterization. *Soft Matter*, 2:310–323, 2006.

K. Ghosh, Z. Pan, E. Guan, S. Ge, Y. Liu, T. Nakamura, Z.-D. Ren, M. Rafailovich, and R.A.F. Clark. Cell adaptation to a physiologically relevant ecm mimic with different viscoelastic properties. *Biomaterials*, 28:671–679, 2007.

A. Goriely and M. Ben Amar. On the definition and moeling of incremental, cumulative, and continuous growth laws in morphelasticity. *Biomechanical Models of Mechanobiology*, 6:289–296, 2007.

H.C. Grillo, G.T. Watts, and J. Gross. Studies in wound healing: I. contraction and the wound contents. *Annals of Surgery*, 148:145–152, 1958.

F. Grinnell, C.-H. Ho, E. Tamariz, D.J. Lee, and G. Skuta. Dendritic fibroblasts in three-dimensional collagen matrices. *Molecular Biology of the Cell*, 14:384–395, 2003.

C.L. Hall. *Modelling of some biological materials using continuum mechanics.* PhD thesis, Queensland University of Technology, 2009.

B.A. Harley, T.M. Freyman, M.Q. Wong, and L.J. Gibson. A new technique for calculating individual dermal fibroblast contractile forces genrated within collagen-gag scaffolds. *Biophysical Journal*, 93:2911–2922, 2007.

B. Hinz. Formation and function of the myofibroblast during tissue repair. *Journal of Investigative Dermatology*, 127:526–537, 2007.

B. Hinz. Tissue stiffness, latent tgf-$\beta$1 activation, and mechanical signal transduction: Implications for the pathogenesis and treatment of fibrosis. *Journal Current Rheumatology Reports*, 11:120–126, 2009.

B. Hinz. The myofibroblast: Paradigm for a mechanically active cell. *Journal of Biomechanics*, 43:146–155, 2010.

B. Hinz and G. Gabbiani. Mechanisms of force generation and transmission by myofibroblasts. *Current Opinion in Biotechnology*, 14:538–546, 2003.

B. Hinz, D. Mastrangelo, C.E. Iselin, C. Chaponnier, and G. Gabbiani. Mechanical tension controls granulation tissue contractile activity and myofibroblast differentiation. *Americal Journal of Pathology*, 159:1009–1020, 2001.

E. Javierre, P. Moreo, M. Doblaré, and J.M. García-Aznar. Numerical modeling of a mechano-chemical theory for wound contraction analysis. *International Journal of Solids and Structures*, 46:3597–3606, 2009.

D.F. Kennedy and W.J. Cliff. A systematic study of wound contraction in mammalian skin. *Pathology*, 11:207–222, 1979.

F. Khatyr, C. Imberdis, P. Vescovo, D. Varchon, and J.-M. Lagarde. Model of the viscoelastic behaviour of skin *in vivo* and the study of anisotropy. *Skin Research and Technology*, 10:96–103, 2004.

M.R. Khorramizadeh, E.E. Tredget, C. Telasky, Q. Shen, and A. Ghahary. Aging differentially modulates the expression of collagen and collagenase in dermal fibroblasts. *Molecular and Cellular Biochemistry*, 194:99–108, 1999.

Y. Kim and A. Friedman. Interaction of tumor with its micro-environment: A mathematical model. *Bulletin of Mathematical Biology*, 2009. Published online.

M.S. Kolodney and R.B. Wysolmerski. Isometric contraction by fibroblasts and endothelial cells in tissue culture: A quantitative study. *The Journal of Cell Biology*, 117:73–82, 1992.

M. Kucharova, S. Ďoubal, P. Lemera, P. Rejchrt, and M. Navrátil. Viscoelasticity of biological materials - measurement and practical impact on biomedicine. *Physiological Research Supplementary 1*, 56:S33–S37, 2007.

B. Li and J.H.-C. Wang. Fibroblasts and myofibroblasts in wound healing: Force generation and measurement. *Journal of Tissue Viability*, 2009. Article in Press, Available Online.

G.M. Luccioli, D.S. Kahn, and H.R. Robertson. Histologic study of wound contraction in the rabbit. *Annals of Surgery*, 160:1030–1040, 1964.

G. Majno and I. Joris. *Cells, Tissues and Diseases - Principles of Gernal Pathology*. Oxford University Press, 2 edition, 2004.

S.K. Masur, H.S. Dewal, T.T. Dinh, I. Erenburg, and S. Petridou. Myofibroblasts differentiate from fibroblasts when plated at low density. *Proceedings of the National Academy of Sciences of the United States of America*, 93:4219–4223, 1996.

M.H. McGrath and J.M. Emery. The effect of inhibition of angiogenesis in granulation tissue on wound healing and the fibroblast. *Annals of Plastic Surgery*, 15:105–122, 1985.

M.H. McGrath and R.H. Simon. Wound geometry and the kinetics of wound contraction. *Plastic and Reconstructive Surgery*, 72:66–72, 1983.

C.J. Morgan and W.J. Pledger. *Wound Healing: Biochemical and Clinical Aspects*, chapter 4, pages 63–76. Saunders, Philadelphia; London, 1992.

V. Moulin, G. Castilloux, A. Jean, D.R. Garrel, F.A. Auger, and L. Germain. In vitro models to study wound healing fibroblasts. *Burns*, 22:359–362, 1996.

V. Moulin, G. Castilloux, F.A. Auger, D.R. Garrel, M.D. O'Connor-McCourt, and L. Germain. Modulated response to cytokines of humand wound healing myofibroblasts compared to dermal fibroblasts. *Experimental Cell Research*, 238:283–293, 1998.

V. Moulin, S. Larochelle, C. Langlois, I. Thibault, C.A. Lopez-Vallé, and M. Roy. Normal skin wound and hypertrophic scar myofibroblasts have differential responses to apoptotic inductors. *Journal of Cellular Physiology*, 198:350–358, 2004.

H. Murata, L. Zhou, S. Ochoa, A. Hasan, E. Badiavas, and V. Falanga. Tgf-$\beta$3 stimulates and regulates collagen synthesis through tgf$\beta$1-dependent

and independent mechanisms. *Journal of Investigative Dermatology*, 108: 258–262, 1997.

J.D. Murray. *Mathematical Biology II: Spatial Models and Biomedical Applications*, volume 18 of *Interdisciplinary Applied Mathematics*. Springer, 3 edition, 2003.

L. Olsen, J.A. Sherratt, and P.K. Maini. A mechanochemical model for adult dermal wound contraction and the permanence of the contracted tissue displacement profile. *Journal of Theoretical Biology*, 17:113–128, 1995.

L. Olsen, J.A. Sherratt, and P.K. Maini. A mathematical model for fibroproliferative wound healing disorders. *Bulletin of Mathematical Biology*, 58:787–808, 1996.

L. Olsen, J.A. Sherratt, and P.K. Maini. A mechanochemical model for normal and abnormal dermal wound repair. *Nonlinear Analysis*, 30:3333–3338, 1997.

L. Olsen, J.A. Sherratt, and P.K. Maini. Spatially varying equilibria of mechanical models: Application to dermal wound contraction. *Mathematical Biosciences*, 147:113–129, 1998.

L. Olsen, P.K. Maini, J.A. Sherratt, and J.C. Dallon. Mathematical modelling of anisotropy in fibrous connective tissue. *Mathematical Biosciences*, 158:145–170, 1999.

S. Ramtani. Mechanical modelling of cell/ecm and cell/cell interactions during the contraction of a fibroblast-populated collagen microsphere: theory and model simulation. *Journal of Biomechanics*, 37:1709–1718, 2004.

S. Ramtani, E. Fernandes-Morin, and D. Geiger. Remodeled-matrix con-

traction by fibroblasts: numerical investigations. *Computers in Biology and Medicine*, 32:283–296, 2002.

R. Reihsner, B. Balogh, and E.J. Menzel. Two-dimensional elastic properties of human skin in terms of incremental model at the *in vivo* configuration. *Medical Engineering and Physics*, 17:3–4–313, 1995.

J.M. Rhett, G.S. Ghatnekar, J.A. Palatinus, M. O'Quinn, M.J. Yost, and R.G. Gourdie. Novel therapies for scar reduction and regenerative healing of skin wounds. *Trends in Biotechnology*, 26:173–180, 2008.

A.B. Roberts, B.K. McCune, and M.B. Sporn. Tgf-$\beta$: Regulation of extracellular matrix. *Kidney International*, 41:557–559, 1992.

D.I. Shreiber, V.H. Barocas, and R.T. Tranquillo. Temporal variations in cell migration and traction during fibroblast-mediated gel compaction. *Biophysical Journal*, 84:4102–4114, 2003.

G.S. Shultz, G. Ladwig, and A. Wysocki. Extracellular matrix: review of its roles in acute and chronic wounds. Published online at World Wide Wounds, URL: http://www.worldwidewounds.com/2005/august/Schultz/Extrace-Matric-Acute-Chronic-Wounds.html, 2005.

A.L. Sillman, D.M. Quang, B. Farboud, K.S. Fang, R. Nuccitelli, and R.R Isseroff. Human dermal fibroblasts do not exhibit directional migration on collagen 1 in direct-current electric fields of physiological strength. *Experimental Dermatology*, 12:396–402, 2003.

F.H. Silver, J.W. Freeman, and D. DeVore. Viscoelastic properties of human skin and processed dermis. *Skin Research and Technology*, 7:18–23, 2001.

A.J. Singer and R.A.F. Clark. Cutaneous wound healing. *The New England Journal of Medicine*, 341:738–747, 1999.

E. Tamariz and F. Grinnell. Modulation of fibroblast morphology and adhesion during collagen matrix remodelling. *Molecular Biology of the Cell*, 13:3915–3929, 2002.

P. Tracqui, D.E. Woodward, G.C. Cruywagen, J. Cook, and J.D. Murray. A mechanical model for fibroblast-driven wound healing. *Journal of Biological Systems*, 3:1075–1084, 1995.

L. Tranqui and P. Tracqui. Mechanical signalling and angiogenesis. the integration of cell-extracellular matrix couplings. *Life Sciences*, 323:31–47, 2000.

R.T. Tranquillo and J.D. Murray. Continuum model of fibroblast-driven wound contraction: Inflammation-mediation. *Journal of Theoretical Biology*, 158:135–172, 1992.

J.S. Vande Berg, R. Rudolph, W.L. Poolman, and D.R. Disharoon. Comparative growth dynamics and activ concentration between cultured human myofibroblasts from granulating wounds and dermal fibroblasts from normal skin. *Laboratory Investigation*, 61:532–538, 1989.

F.J. Vermolen and E. Javierre. Computer simulations from a finite-element model for wound contraction and closure. *Journal of Tissue Viability*, 19: 43–53, 2010.

J.E. Wagenseil and R.J. Okamoto. Modeling cell and matrix anisotropy in fibroblast populated collagen vessels. *Biomechanics and Modeling in Mechanobiology*, 6:151–162, 2007.

T. Wakatsuki, M.S. Kolodney, G.I. Zahalak, and E.L. Elson. Cell mechanics studied by a reconsituted model tissue. *Biophysical Journal*, 79:2353–2368, 2000.

G.T. Watts. Wound shape and tissue tension in healing. *The British Journal of Surgery*, 47:555–561, 1960.

R.G. Wells and D.E. Discher. Matrix elasticity, cytoskeletal tension, and tgf$\beta$: The insoluble and soluble meet. *Science Signaling*, 1:pe13, 2008.

P.-J. Wipff and B. Hinz. Myofibroblasts work best under stress. *Journal of Bodywork and Movement Therapies*, 13:121–127, 2009.

L.K. Wrobel, T.R. Fray, J.E. Molloy, J.J. Adams, M.P. Armitage, and J.C. Sparrow. Contractility of single human dermal myofibroblasts and fibroblasts. *Cell Motility and the Cytoskeleton*, 52:82–90, 2002.

L. Yang, C.X. Qiu, A. Ludlow, M.W.J. Ferguson, and G. Brunner. Active transforming growth factor-$\beta$ in wound repair: Determination using a new assay. *American Journal of Pathology*, 154:105–111, 1999.

G.I. Zahalak, J.E. Wagenseil, T. Wakatsuki, and E.L. Elson. A cell-based constitutive relation for bio-artificial tissues. *Biophysical Journal*, 79: 2369–2381, 2000.

## Appendix A. Variable and Parameter Names

The following are the variables with their names as used in the model:

- $n$: Fibroblast density inside the wound
- $m$: Myofibroblast density inside the wound
- $s$: Collagen density inside the wound
- $e$: Effective strain inside the wound
- $S$: Collagen density outside the wound

- $E$: Effective strain outside the wound
- $L$: Distance of wound boundary from wound center

Table A.1 lits the parameters prior to non-dimensionalization together with their names and units.

| Parameter | Name | Units |
|---|---|---|
| $R$ | Ingress of fibroblasts | cm/day |
| $g$ | Fibroblast proliferation | 1/day |
| $r$ | Fibroblast activation to myofibroblasts | 1/N.$(\mu$g$)^2$.day |
| $a$ | Myofibroblast apoptosis | 1/day |
| $b$ | TGF$\beta$ decay | 1/day |
| $k_1$ | Collagen production | $\mu$g/cell.day |
| $k_2$ | Collagen degradation | 1/cell.day |
| $\eta$ | Relative collagen production by myofibroblasts | U |
| $\delta$ | Relative collagen degradation by myofibroblasts | U |
| $k_\zeta$ | Contractile strain produced by fibroblasts | 1/cells.$\mu$g.day |
| $k_\rho$ | Matrix turnover by fibroblasts | $\mu$g/cells.day |
| $\pi_\zeta$ | Myofibroblast to fibroblast contractile strain generation | U |
| $\pi_\rho$ | Myofibroblast to fibroblast remodelling | U |
| $Y$ | Elastic modulus | N |
| $\tau$ | Fibroblast cell traction | N/cell |
| $\zeta$ | Myofibroblast to fibroblast cell traction | U |

Table A.1: Table of parameters names and units. U refers to a parameter with unit dimension.

## Appendix B. Parameter Estimates and Non-Dimensionalisation

Accurate parameter estimation is always an essential component of the modelling process. In view of this, it is important to state any simplifying assumptions before discussing parameter values. In our case:

- The proportionality constants for myofibroblast to fibroblast collagen production and degradation are assumed to be equal, and we set $\eta = \delta$.
- The proportionality constant for myofibroblast to fibroblast matrix turnover is assumed to be the same as that of myofibroblast collagen production, since these processes are essentially the same. Hence we set $\pi_\rho = \eta$.

Before considering the remaining parameters, we estimate values for the scalings used to non-dimensionalise the variables (see below).

$\alpha$: A typical length scale for acute dermal wounds is 1cm.

$g$: It was chosen to scale time relative to fibroblast proliferation. Alberts et al. (1989), Morgan and Pledger (1992) and Ghosh et al. (2007) state that the average doubling time for for fibroblasts is approximately $18-20$ hours. This gives a range for the proliferation rate of $0.832 < g < 0.924$, which is consistent with curve fitting estimates for cell growth from Khorramizadeh et al. (1999). We choose the lower limit, and so $g = 0.832$/day.

$\hat{N}$: The carrying capacity of fibroblasts is known to be approximately $10^6$/mL (Vande Berg et al., 1989). Hence, we take $\hat{N} = 10^6$cells/mL.

$k_1/k_2$: It is known that 30% of newly synthesized collagen is degraded (Aumailley et al., 1982). Hence, $k_2 = 0.3k_1$, such that $k_1/k_2 = 3.33$. The value for $k_1$ was chosen following order of magnitude approximations using nu-

merical simulations, and was found to be approximately $0.1 - 1\mu$g/cell.day.

$\beta_0$: Yang et al. (1999) found the initial concentration of TGF$\beta$ in the wound to be 0.275ng/cm$^3$. Hence, we take $\beta_0 = 0.275$ng/cm$^3$.

We can now apply the following non-dimensionalisation:

$$\bar{L} = \frac{L}{\alpha}, \quad \bar{t} = gt, \quad \bar{n} = \frac{n}{\hat{N}}, \quad \bar{m} = \frac{m}{\hat{N}}, \quad \bar{s} = \frac{k_2 s}{k_1}, \quad \bar{S} = \frac{k_2 S}{k_1},$$
$$\bar{e} = e, \quad \bar{E} = E, \quad \hat{\beta} = \frac{\beta}{\beta_0}$$

The values for the remaining dimensional parameters are as follows.

$R$: Experiments by Sillman et al. (2003) on collagen I found that fibroblasts derived from normal human dermal wounds migrate at an average velocity of $0.23 - 0.36\mu$m/min. This gives a range of $0.033 < R < 0.052$cm/day. We choose the lower limit of $R = 0.033$cm/day.

$r$: Desmouliere et al. (1993) found that culturing fibroblasts in the presence of TGF$\beta$ increased the percentage of cells expressing $\alpha$-SMA from 7.5% to 45.3%, representing an activation of 37.8% of fibroblasts. This is consistent with other estimates (Masur et al., 1996; Moulin et al., 1996). The Desmouliere experiment took place over a one week period, yielding an approximation of $r \approx 0.054$/day.

$Y$: Estimates of $Y$ range from $10 - 300$N/cm$^2$ (Silver et al., 2001; Genzer and Groenewold, 2006). We consider an area of approximately 1cm$^2$, which gives a range of $Y$ of $10 < Y < 300$N. We use the estimate by Ahlfors and Billiar (2007) of 71.3N/cm$^2$, such that $Y = 71.3$N.

$a$: Moulin et al. (2004) estimate that $8 - 20\%$ of myofibroblasts undergo apoptosis. Hence, we choose $a = 0.2$/day.

$b$: The TGF$\beta$ decay rate was estimated from the exponential phase of the data from Yang et al. (1999), giving a rate of $b \approx 0.354$/day.

$\eta$, $\delta$: On a percentage basis, myofibroblasts produce roughly twice the collagen that is synthesized by fibroblasts (Olsen et al., 1995; Moulin et al., 1998; Kim and Friedman, 2009). Hence, we choose $\eta = \delta = 2$.

$k_\zeta$, $k_\rho$: During the non-dimensionalisation, it was seen that $k_\zeta$ and $k_\rho$ are both proportional to fibroblast synthesis. Further, since strain must be small, this implies $k_\zeta \ll k_\rho$. Based on this, we choose $k_\zeta = k_\rho/100$.

$\pi_\zeta$: This value is unknown. However, since myofibroblasts are much stronger than fibroblasts, we suggest that $\pi_\zeta$ is approximately $O(10)$.

$\tau$: Values for $\tau$ differ by several orders of magnitude. By comparing some reported experimental values and values used in other models of dermal repair, it seems realistic to take $\tau = 2\mu\text{N/cell}$. This is consistent with Fray et al. (1998) and Wrobel et al. (2002).

$\zeta$: Myofibroblasts are known to perform the majority of wound contraction, and so a value of $\zeta = 5$ was chosen (Olsen et al., 1995; Javierre et al., 2009).

Finally, the following non-dimensionalisation is used.

$$\tilde{R} = \frac{R}{\alpha g}, \qquad \tilde{r} = \frac{rK_{1n}}{gK_{2n}}, \qquad \tilde{Y} = Y, \qquad \tilde{a} = \frac{a}{g}, \qquad \tilde{b} = \frac{b}{g}$$
$$\kappa = \frac{K_{2n}\hat{N}}{g}, \quad \tilde{\eta} = \eta = \delta = \pi_\rho, \quad \tilde{k}_\rho = \frac{k_\rho \kappa}{k_1}, \quad \tilde{k}_\zeta = \frac{k_\zeta k_1 \kappa}{k_2^2}, \quad \tilde{\pi} = \pi_\zeta$$
$$\tilde{\tau} = \tau\hat{N}, \qquad \tilde{\zeta} = \zeta.$$

# RECENT REPORTS

| | | |
|---|---|---|
| 23/11 | Positive or negative Poynting efect? The role of adscititious inequalities in hyperelastic materials | Mihai<br>Goriely<br>McCue<br>McElwain |
| 24/11 | On approaches to modelling lattice dislocations | Hall<br>Markenscoff |
| 25/11 | Nonlinear waves in heterogeneous elastic rods via homogenization | de Luna<br>Emptage<br>Goriely<br>Bressloff |
| 26/11 | Synaptic bistability due to nucleation and evaporation of receptor clusters | Burlakov<br>Duričković<br>Goriely |
| 27/11 | Particle trapping and banding in rapid solidification | Elliot<br>Peppin |
| 28/11 | Growth of confined cancer spheroids: a combined experimental and mathematical modelling approach | Loessner<br>Flegg<br>Byrne<br>Hall<br>Moroney<br>Clements<br>McElwain<br>Hutmacher |
| 29/11 | Floating carpets and the delamination of elastic sheets | Wagner<br>Vella |
| 30/11 | Numerical Study of Liquid Crystal Elastomers by a Mixed Finite | Luo<br>Calderer |
| 31/11 | The indentation of pressurized elastic shells: From polymeric capsules to yeast cells | Vella<br>Ajdari<br>Vaziri<br>Boudaoud |
| 32/11 | Wrinkling of pressurized elastic shells | Vella<br>Ajdari<br>Vaziri<br>Boudaoud |
| 33/11 | Data assimilation using bayesian filters and B-spline geological models | Duan<br>Farmer<br>Hoteit<br>Lu<br>Moroz |
| 34/11 | Review of nonlinear Kalman, ensemble and particle filtering with application to the reservoir history matching problem | Luo<br>Hoteit<br>Duan<br>Wang |
| 35/11 | Modelling a Tethered Mammalian Sperm Cell undergoing Hyperactivation | Curtis<br>Kirkman-Brown<br>Connolly |

| | | |
|---|---|---|
| 39/11 | An asymptotic theory for the re-equilibration of a micellar surfactant solution | Griffiths<br>Bain<br>Breward<br>Chapman<br>Howell<br>Water |
| 40/11 | Higher-order numerical methods for stochastic simulation of chemical reaction systems | Székely<br>Burrage<br>Erban<br>Zygalakis |
| 41/11 | On the modelling and simulation of a high pressure shift freezing process | Smith<br>Peppin<br>Ángel M. Ramos |
| 42/11 | An efficient implementation of an implicit FEM scheme for fractional-in-space reaction-diffusion equations | Burrage<br>Hale<br>Kay |
| 43/11 | Coupling fluid and solute dynamics within the ocular surface tear film: a modelling study of black Line osmolarity | Zubkov<br>Breward<br>Gaffney |
| 44/11 | A prototypical model for tensional wrinkling in thin sheets | Davidovitch<br>Schroll<br>Vella<br>Adda-Bedia<br>Cerda |
| 45/11 | A fibrocontractive mechanochemical model of dermal wound closure incorporating realistic growth factor | Murphy<br>Hall<br>Maini<br>McCue<br>McElwain |

**Copies of these, and any other OCCAM reports can be obtained from:**

**Oxford Centre for Collaborative Applied Mathematics**
**Mathematical Institute**
**24 - 29 St Giles'**
**Oxford**
**OX1 3LB**
**England**
**www.maths.ox.ac.uk/occam**